1 MHz akinetic dispersive ring cavity swept source at 850 nm

Florin Toadere[1], Radu-F. Stancu[1], Wallace Poon[2], David Schultz[2], Adrian Podoleanu[1]

Abstract - A fast dual mode-locked akinetic optical swept source at 850 nm central wavelength is presented using a dispersive cavity. We demonstrate that single mode fiber can be successfully used as dispersive element to induce mode locking. A first locking condition is imposed by driving the optical gain at a high frequency, to induce mode locking, while a second locking condition involves sweeping at a rate close to resonance value. In this regime, using the same fiber length in the loop, sweeping rates of 0.5 MHz and 1 MHz are demonstrated with proportional reduction in the tuning bandwidth. The axial range of the swept source was evaluated by scanning through the channeled spectrum of a Michelson interferometer.

Index Terms—Semiconductor optical amplifier, laser mode locking, ring laser, optical fiber dispersion, radio frequency.

I. Introduction

The majority of commercial OCT systems for retina imaging operate in the 800 – 900 nm band using spectrometer based OCT principle [1], [2]. There is a trend in equipping commercial systems for ophthalmology with swept sources, due to longer axial range and better sensitivity, however fast sweeping rates are available at longer wavelengths only. At shorter wavelength, transversal resolution is better and the 800 nm band is also suitable for oxygenation measurements. Therefore, a continuous interest exists in developing swept sources at a 850 nm central wavelength.

Development of fast swept sources (SS) focused on opto-mechanical principles of tuning applied to a closed loop laser cavity. To exemplify, the following devices were employed: a Fabry-Perot filter [4], a polygon filter [5], or a micro electrical mechanical scanning (MEMS) device [6,7]. These opto-mechanical elements can exhibit hysteresis and are strongly influenced by electrical instabilities. An alternative in the technology of swept sources for OCT consists in the elimination of the mechanical tuning elements from the laser cavity [8], to achieve akinetic operation. Another akinetic principle is based on dispersion tuning [9-12]. We have demonstrated recently an improvement to this concept, represented by dual resonance excitation [13]. A first resonance condition is imposed by driving the optical gain at a multiple of the cavity resonance frequency, f_R, to induce mode-locking. The second mechanism is responsible for generating sweeping at a rate close to f_R, more exactly at values detuned from f_R [9]. So far, this dual resonance mechanism was proven at wavelengths longer than 1 μm. In this paper, the concept of dual mode-locking and dispersion tuning is extended to the 850 nm band. In comparison with previous implementations, we demonstrate that the dispersion of single mode fiber at 850 nm, used as the necessary delay element, is sufficient to act as dispersive element for the principle illustrated. At longer wavelengths, other dispersive elements have been reported, such as dispersive compensating fiber [9,10,13] or chirped fiber Bragg gratings [11]. MHz sweeping is reported with sufficient narrow linewidth (90 pm) and tuning bandwidth over 10 nm.

II. Dual mode-locking

The operation of mode-locking dispersion ring cavity akinetic swept source (AKSS), sweeping at hundreds of kHz was presented in several reports [9-13]. The resonance frequency of the ring laser cavity is defined as:

$$f_r = \frac{c}{nL} \tag{1}$$

where: c represents the speed of light in vacuum, n is the refractive index of the cavity and L is the laser cavity length. f_R denotes the spacing between adjacent modes in a resonant cavity. Mode locking is induced by modulating the semiconductor optical amplifier (SOA) at a frequency f_{m0}, that is a multiple, N, of the frequency f_r, e.g. Nf_R. Mode-locking allows obtaining ultrashort laser pulses at the SOA output. Thus, SOA operates at a wavelength that fulfills the mode-looking condition. The wavelength tuning range $\Delta\lambda$ is given by:

$$\Delta\lambda = -\frac{n_0}{cDf_{m_0}}\Delta f_m \tag{2}$$

where f_{m0} is the central mode-locking frequency, n_0 is the refractive index at central optical frequency, D is the dispersion parameter of the ring, and Δf_m represents the change in modulation frequency. When Δf_m reaches the resonance frequency, the maximum tuning range $\Delta\lambda_{max}$ is achieved:

$$\Delta\lambda_{max} = \frac{1}{|D|Lf_{m0}} \tag{3}$$

The frequency of the RF signal is changed within the bandwidth Δf_m using a voltage controlled oscillator (VCO). When the frequency of the signal driving the VCO is swept at $f_s = f_R$, the VCO's spectrum is described by a comb of frequencies $f_{m0} \pm f_R$,

Paper submitted on: 01/11/2016. Radu-F. Stancu, Florin Toadere, Adrian Gh. Podoleanu are with the Applied Optics Group, School of Physical Sciences, University of Kent, Canterbury, United Kingdom, CT2 7NH (e-mail: rs672@kent.ac.uk, ap11@kent.ac.uk). Wallace Poon and David Schultz are with the East Kent Hospital University NHS Foundation Trust. A. P. was supported by the Royal Society Wolfson Research Merit Award and by the BRC-UCL at Inst. of Ophthalmology London; F.T was supported by Univ. of Kent; R.-F. S. was supported by the Brilliant Club Researchers in Schools Programme; F.T. and R-F. S. have equally contributed to the paper.

$f_{m0} \pm 2f_R$, $f_{m0} \pm 3f_R$, and so on. Under these conditions, each component of the comb differs from f_{m0} by a multiple of f_R and therefore all comb components determine the same laser optical frequency, repeated at f_R. Therefore, to obtain optical tuning, the frequency of the signal driving the laser has to be detuned from resonance. For a detuning δf_R, with $f_s = f_R \pm \delta f_R$, the spectrum of the VCO is a comb spectrum consisting in f_{m0}, $f_{m0} \pm f_R \pm \delta f_R$, $f_{m0} \pm 2f_R \pm 2\delta f_R$, $f_{m0} \pm 3f_R \pm 3\delta f_R$ and so on. The step δf_r of the radiofrequency determines a change in wavelength $\delta\lambda$. In such case, the output bandwidth $\Delta\lambda$ is given by:

$$\Delta\lambda = \frac{\Delta F}{f_r} \cdot C_m \cdot \delta f_r \cdot \delta\lambda \quad (4)$$

where C_m is a coefficient and ΔF represents the frequency tuning range of the VCO. The step change in wavelength $\delta\lambda$ can be assimilated to the linewidth of the optical emission.

The optical configuration of the AKSS experimented is shown in Fig. 1. It uses a SOA model SOA-372, operating at 850 nm, maximum current 200 mA and 3 dB bandwidth up to 40 nm. The SOA is placed in a laser system mount model HS501, and it is driven by a Thorlabs LDC 210C power supply. Temperature stability is ensured through thermo-electric cooling provided by a Thorlabs TEC 200C driver (sensor TH 20kΩ). The SOA is delimited by two polarization insensitive isolators IO-F-SLD 100-840 which ensure unidirectional lasing. Output power is drawn out via a 50/50 FOC Photonics coupler with the central wavelength 850 nm, with 50% of power reinjected in the cavity.

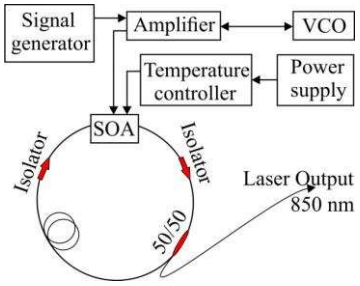

Fig. 1. Akinetic swept source schematic diagram

The output spectra of the SS configuration are measured using a Yokogawa AQ6375 optical spectrum analyzer (OSA). The coherence length of the source is evaluated by feeding a balanced interferometer, equipped with a spectral delay line for dispersion adjustment, terminated on a 50/50 SIFAM 01035834 coupler with the central wavelength 850 nm, ending on a New Focus balanced detector model 1807, 80 MHz, 320-1000 nm bandwidth, whose output is displayed with a LeCroy Wave Runner 104 MXi-A 1GHz oscilloscope, at a sampling rate of 10 GS/s (Gyga Sample points/ second). In dynamic regime, a ZX-95-928CA-S+ Mini Circuits low noise VCO and a ZHL-42W Mini Circuits radio frequency amplifier are used to drive the SOA. The VCO is driven by a ramp signal generated by an Agilent 81160A radio frequency signal generator (RFSG), with adjustable amplitude, frequency and offset. The offset of the ramp signal determines the central mode-locking frequency f_{mo} generated by the VCO and its amplitude sets the tuning bandwidth ΔF of the VCO. The repetition frequency of the ramp signal determines the tuning rate f_s. Then the VCO's signal is amplified by the radio frequency amplifier before it is delivered to SOA. By changing the frequency of the VCO signal, the SOA optical frequency is swept. Empirically it was noted that ramps driving the optical frequency from high to low leads to a larger tuning bandwidth and a better signal to noise ratio than ramps driving the optical frequency from low to high. This is in line with previous observations in FDML lasers [14].

III. Experimental results

A Hewlett Packard 8648C RFSG, operating in the 9 kHz - 3200 MHz frequency band, was employed in the measurements performed in the static regime (manually adjusting the mode-locking frequency). The amplitude of signal at the SOA driver input is 15 V at 250 MHz and 12 V at 1 GHz. At larger frequencies, although the generator output was increased, no change was noticed in the spectrum, suggesting that the power amplifier worked in saturation regime. However, we cannot measure the exact current swing through the SOA due to limitation of our electronic bandwidth (photodetector and oscilloscope). Inside the driver, there is a serial resistance of 33 Ω in series with the SOA, determining a load of approximately 50 Ω. The cavity dispersion was adjusted by modifying the length of the resonant cavity. Thus, four types of single mode fibers are tested as listed in Table 1. For all four configurations the resonance frequencies are listed in the 3rd column of Table 1. As expected, the larger the length of the cavity, less is the resonance frequency. The fourth and fifth columns list the optical bandwidth and respectively, the tuning of the f_{m0} range to generate the output bandwidth, for a mode-locking frequency f_{mo} = 1 GHz. The widest tuning bandwidth was achieved when using fiber F2.

Table 1. Static regime of the resonant cavity

Fiber type	Cavity length [m]	Resonance f_r [kHz]	$\Delta\lambda_{max}$ [nm]	Δf_s [kHz]
F1: SM 780/125 A	107	1864	8	150
F2: Thorlabs FS-SN-4224	108	1853	14	255
F3: Lightwave Tech. Inc., F1506C	400	499.5	9	230
F4: Ensign Bickford SMC A0820B	700	281.4	9	160

Fig. 2 (left) illustrates the static bandwidth for two different values of the RF frequency, f_{m0}. By varying the RF to either extremity of the RF bandwidth, two optical frequency components are seen. This proves that Δf_m reaches the resonance frequency condition, that lead to Eq (3).

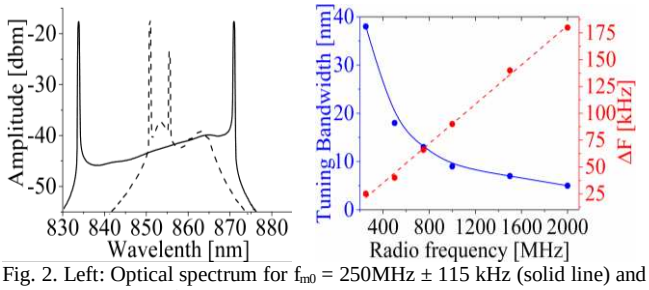

Fig. 2. Left: Optical spectrum for f_{m0} = 250MHz ± 115 kHz (solid line) and f_{m0} = 2GHz ± 125 kHz for (dashed line); Right: Maximum tuning bandwidth (blue solid line) and the radio frequency tuning range ΔF (dashed red line) necessary to achieve $\Delta\lambda$ = 4 nm versus the frequency of the mode-locking frequency, f_{m0}.

Table 2 presents several measurements of the wavelengths and linewidths obtained in static regime employing a 400 m ring cavity. The central mode-locking frequency f_{m0} inducing the mode locking is varied from 250 MHz to 2 GHz. For each value of f_{m0}, its frequency was statically modified and the optical frequency determined by the change was followed in its variation using the optical spectrum analyzer. The maximum bandwidth values obtained, $\Delta\lambda_{max}$, are listed in the second column, while the linewidths measured are shown in the third column. The number of points in the spectrum are calculated in the fourth column, by dividing the maximum optical tuning bandwidth to the value of linewidth. Because this is measured for a static condition, where the frequency of the VCO is held fixed, we refer to such linewidth as static, $\delta\lambda_{st}$ This is the minimum achievable linewidth and should be distinguished from the step $\delta\lambda$ used in Eq. (4) in dynamic regime. In the fifth column, the values of the dispersion parameter D are calculated using Eq. (3). These give an average value D = 199 [ps/nm/km]. The RF deviations that created these optical tuning bandwidths are mentioned in the sixth column.

Table 2. Measured parameters of the AKSS employing a 400 m Lightwave Technologies, F1506C fiber ring cavity

f_{m0} [MHz]	$\Delta\lambda_{max}$ [nm]	$\delta\lambda_{st}$ [nm]	$\Delta\lambda_{max}/\delta\lambda_{st}$	D [ps/nm/km]	Δf_m [kHz]
250	50	0.12	417	200	230
500	28	0.1	280	179	230
750	20	0.09	222	166	240
1000	13	0.08	163	192	230
1500	8	0.08	100	208	250
2000	5	0.08	63	250	250

Then we maintained the maximum frequency of 2 GHz of the signal applied to the SOA and changed the fiber. The narrowest static linewidths $\delta\lambda_{st}$ of 70 pm are achieved using F3 and F4. Larger static linewidths of 130 pm and 120 pm are obtained using the fiber F1 and, respectively, F2. For the linewidth measurements, the OSA was adjusted on a resolution of 20 pm. These measurements refer to the width of envelope emission over many optical modes, impacting both the sensitivity decay with the path difference in the interferometer and what can be effectively measured with an OSA.

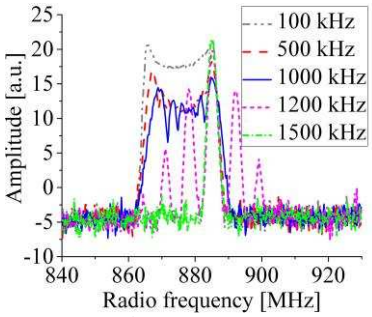

Fig. 3. Amplitude versus radio frequency applied to VCO

Understanding the RF spectrum is important, as each RF component in the spectrum determines an optical frequency, as described by equation (4). At 1500 kHz tuning rate, only a single peak is left in the RF spectrum in Fig. 3. According to the theory of frequency modulation, the index of modulation is the ratio of $\Delta F/f_m$. For the data in Fig. 2 (left), using 60 MHz/f_m, suggests that even at 1 MHz, the index is larger than 1. This means that the radio frequency spectrum consists of more components than J1 (integer number Bessel function first order). At 1.2 MHz these multiple components can be resolved by the RFSA. According to Table 2, when using the VCO close to 1 GHz, if the RF is varied by 230 kHz, then a tuning bandwidth of 13 nm should be achievable.

Next, the dynamic regime operation of the source is characterized. A sinusoidal wave produced by the RSFG is applied to the VCO and the RF spectrum is measured using an Agilent RF Spectrum analyzer. The VCO operation is tested with signals of repetition frequency between 100 kHz to 1500 kHz and amplitude kept constant at 5 V. According to the VCO data sheet, this amplitude should produce a tuning of 100 MHz.

Dynamically, the laser optical output is tuned according to two interleaved mechanisms, as previously communicated [8, 9]. A first mechanism is that of dispersive tuning. The second tuning mechanism involves resonance tuning using the cavity roundtrip; the tuning must be slightly detuned from the cavity resonance. We show the effects obtained for seven such steps, where each step is δf_R = 500 Hz. For $f_S = f_R - 500$ Hz, the VCO frequency contains the following components: f_{m0} to $f_{m0} - f_R - 500$ Hz, $f_{m0} - 2f_R - 1$ kHz, $f_{m0} - 3f_R - 1.5$ kHz and so on, in the 902 - 928 MHz range, in steps of 999.5 kHz. The emitted spectrum consists of a comb having a linewidth of 80 pm and a repetition rate of 999.5 kHz. For a 3.8 Vpp signal driving the VCO and a laser driving current of 50 mA the output power of the AKSS is 1.6 mW. The 3.8Vpp determines a VCO tuning bandwidth of 60 MHz.

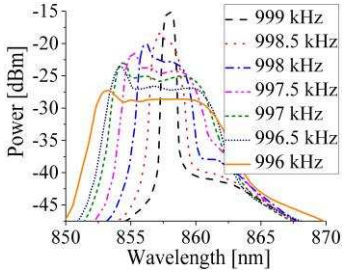

Fig. 4. Optical spectra at the SS output measured for seven values of detuning of the sweeping frequency starting from resonance

By modulating the VCO at sweeping rates of 999 kHz, 998.5 kHz, 998 kHz, and so on, down to 996 kHz, in steps of 0.5 kHz, the measured output bandwidths are: 1.3 nm, 2.5 nm, 4.5 nm, 7.5 nm, 10 nm, 11 nm and, respectively 13.5 nm. This is illustrated in Fig. 4. For an OPD = 50 µm, for each step of detuning the frequency of the VCO by 500 Hz, a new peak is observed in each channeled spectrum at the interferometer output (seen on the oscilloscope screen, not shown here) in addition to the previously existing peaks.

While the tuning bandwidth increases, the optical power decreases, due to driving the laser away from the round trip resonance. The effects of tuning on the output optical power are better documented in Fig. 5. Fig. 5 (left) illustrates the output power versus amplitude of the ramp signal applied to the VCO's input for a detuning of δf_R = 3 kHz when operating the AKSS dynamically at a 996 kHz sweep rate. The larger the

amplitude of the ramp driving the VCO, the larger the tuning bandwidth. On the other hand, a decrease in power is noticeable. Fig. 5 (right) depicts the optical tuning bandwidth and the output power versus the repetition rates around the central resonance of 999 kHz. The larger the detuning from the resonance frequency, the wider the bandwidth and the lower the optical power. A maximum power of 1.6 mW is achieved at the output, without using a booster. Furthermore, the AKSS output was connected to a Michelson interferometer and used the following formulae to determine the useful power of the swept source (P_{SS}) and the ASE power (P_{ASE}), based on the optical power measured in the reference and, respectively, object arm: $P_{obj} = O \cdot (P_{SS} + P_{ASE})$, $P_{ref} = R \cdot (P_{SS} + P_{ASE})$, where: O represents the object arm coefficient, R represents the reference arm coefficient. From the two equations above, the interference power is obtained as: $int = \sqrt{OR} P_{SS}$. Using the method described above, it was concluded that the useful swept source output power represents 20% of the total output power.

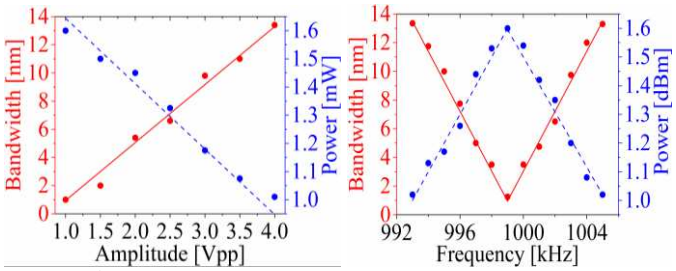

Fig. 5. (left) Output power (dashed blue line) and tuning bandwidth (red solid line) versus the amplitude of the ramp signal applied to the VCO input for δf_R = 3 kHz; (right) tuning bandwidth (red solid line) and optical power (dashed blue line) versus the AKSS repetition rate

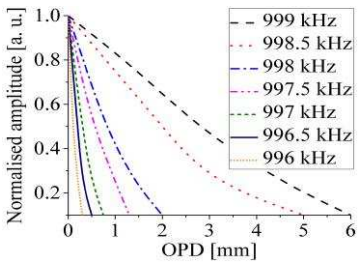

Fig. 6. Amplitude decay of the photo-detected signal with OPD (roll off) for seven detuning values of the sweeping frequency f_S detuned from f_R = 999.5 kHz.

The sensitivity S of the interferometer, in case is used for reflectivity measurement, is calculated as $S = 20log\left(\frac{A_{OPD}}{A_{noise}}\right)$, where A_{OPD} is amplitude of the FFT peak for an OPD close to 0, while A_{noise} represents the amplitude of the noise floor measured outside the peak [15]. S = 88.5 dB is obtained for an OPD value of 0.1 mm. The shape for the spectrum emission is assumed Gaussian and using the OPD_{6dB} worked out from Fig. 6 of 1 mm (obtained for 2 kHz detuning, i.e. the 998 kHz curve), a dynamic linewidth of $\delta\lambda_{dyn} = \frac{\lambda^2}{4 \cdot OPD_{6dB}}$ = 90.31 pm results. This is slightly larger than the static linewidth measured in Table 2, of 80 pm. As the sweeping speed increases, the A-scans showed a decrease in the axial range (OPD). This can be explained by a decrease in the swept source coherence length with the sweeping speed, due to the decrease of roundtrip in the cavity, as it was previously shown in [16]. However sufficient amplitude is obtained up to 6 mm for less detuning, as shown by the curves for 998.5 and 999 kHz in Fig. 4 and Fig. 6.

IV. Conclusion

In this paper, an 850 nm central wavelength AKSS swept at 1 MHz, with over 1 mW power is demonstrated. At a sweeping rate of 998.5 kHz, determining a 4 nm tuning bandwidth, the OPD for 6 dB decay in the interferometer signal is 1 mm. The versatility of this source comes from the possibility of dynamically adjusting their tuning parameters. There is a large ASE power that limits the effectiveness of employing a booster. With more work on the electronic circuitry to secure enhanced mode locking, that couples more modes in the cavity, it is expected to shift more power from the ASE towards the swept frequency components.

References

[1] M. Wojtkowski, R. Leitgeb, A. Kowalczyk, T. Bajraszewski and A. F. Fercher,"In vivo human retinal imaging by Fourier domain optical coherence tomography", J. Biomed. Opt., 7(3), 457-463, (2002).
[2] www.meditec.zeiss.com/cirrus
[3] http://www.optovue.com/products/avanti/
[4] I. Trifanov, A. Bradu, L. Neagu, P. Guerreiro, A. B. Lobo Ribeiro and A. Gh. Podoleanu., "Experimental method to find the optimum excitation waveform to quench mechanical resonances of Fabry–Pérot tunable filters used in swept sources," IEEE Phot. Tech. Lett. 23(12), 825–827 (2011).
[5] S. H. Yun, G. Boudoux, G. J. Tearney, B. E. Bouma, "High-speed wavelength-swept semiconductor laser with a polygon-scanner-based wavelength filter", Optics Letters 28, 1981-1983 (2003)
[6] J. Masson, R. St-Gelais, A. Poulin, Y.-A. Peter, "Tunable Fiber Laser Using a MEMS-Based In Plane Fabry-Pérot Filter", IEEE Journal of Quantum Electronics 46, 1313-1319, (2010).
[7] B. Potsaid et al., "MEMS tunable VCSEL light source for ultrahigh speed 60 kHz-1 MHz axial scan rate and long range centimeter class OCT imaging," Proc. SPIE, 8213, 82130M-8 (2012).
[8] T-H Tsai, B. Potsaid, Y. K. Tao, V. Jayaraman, J. Jiang, P. J. S. Heim, M. F. Kraus, C. Zhou, J. Hornegger, H. Mashimo, A. E. Cable and J. G. Fujimoto, "Ultrahigh speed endoscopic optical coherence tomography using micro-motor imaging catheter and VCSEL technology" Proc. SPIE, 8571, 85710N (2013).
[9] Y. Nakazaki and S. Yamashita, "Fast and wide tuning range wavelength-swept fiber laser based on dispersion tuning and its application to dyamic FBG sensing", Opt. Exp. 17(10), 8310-8318 (2009).
[10] S. Yamashita, Y. Nakazaki, R. Konishi, O. Kusakari, "Wide and fast wavelength-swept fiber laser based on dispersion tuning for dynamic sensing", Journal of Sensors 2009, A Special Issue on Fiber and Integrated Waveguide-Based Opt. Sens., 572835 (2008).
[11] Y. Takubo and S. Yamashita, "High-speed dispersion-tuned wavelength-swept fiber laser using a reflective SOA and a chirped FBG", Optics Express, vol.21, no.4, pp.5130-5139, (2013).
[12] R. F. Stancu, D. A. Jackson and A. G. Podoleanu, "Versatile Swept Source with Adjustable Coherence Length", IEEE Photonics Technology Letters 26 (16), 1629-1632 (2014).
[13] R. F. Stancu and A. G. Podoleanu, "Dual-mode-locking mechanism for an akinetic dispersive ring cavity swept source", Opt. Lett. 40(7), 1322-1325 (2015).
[14] R. Huber, M. Wojtkowski and J.G. Fujimoto, "Fourier Domain Mode-locking (FDML): A new laser operating regime and applications for optical coherence tomography", Optics Express 14(8), 3225-3237 (2006).
[15] A. Gh. Podoleanu and A. Bradu, "Master-Slave interferometry for parallel spectral domain interferometry sensing and versatile 3D optical coherence tomography", Optics Express, Vol. 21, No. 16, 19324-19338 (2013).
[16] A. Takada, M. Fujino, S. Nagano, "Dispersion dependence of linewidth in actively mode-locked ring lasers", Opt. Exp. 20, 4753 (2012).